

Modeling of octave-spanning Kerr frequency combs using a generalized mean-field Lugiato-Lefever model

Stéphane Coen,* Hamish G. Randle, and Miro Erkintalo

Physics Department, The University of Auckland, Private Bag 92019, Auckland, New Zealand

*Corresponding author: s.coen@auckland.ac.nz

Compiled November 1, 2018

We model Kerr frequency combs with a generalized Lugiato-Lefever equation combined with a Newton-Raphson solver. Results in excellent agreement with past experiments are obtained much faster than with any other technique, and we simulate for the first time to our knowledge an octave-spanning Kerr frequency comb. Our study reveals that Kerr combs are associated with temporal cavity solitons and dispersive waves, and opens up new avenues for the understanding of comb formation in ring resonators. © 2018 Optical Society of America

OCIS codes: 230.5750, 190.5530, 190.4380

First observed in 2007, frequency comb generation in monolithic microring resonators has aroused significant research interest [1, 2]. A minuscule footprint, power efficiency, and CMOS-compatibility make said structures ideal for on-chip frequency comb generation. Applications range from spectroscopy to telecommunications.

Although comb generation in ring resonators has been extensively reported experimentally, theoretical studies are comparatively scarce. In part this deficiency can be linked to the intractable computational complexity of the existing models. Indeed, the use of a nonlinear Schrödinger (NLS) equation and appropriate coupling-mediated boundary conditions requires hundreds of millions of roundtrips for convergence, owing to the exceedingly high Q of the structures [3]. Likewise the number of four-wave mixing-mediated coupling terms in coupled mode equation models scales cubically with the number of modes, limiting such modeling to narrowband combs [4]. Matsko *et al.* [5] also considered an analytic approach but it is restricted to resonators of infinite Q-factor and with group-velocity dispersion (GVD) limited to 2nd order. Clearly, a growing demand exists for realistic yet computationally efficient methods for the modeling of frequency combs in high-Q resonators.

In this Letter we report on direct numerical modeling of Kerr frequency combs using a generalized Lugiato-Lefever (LL) equation [6], and find good agreement with reported experiments. Significantly, the conducted computations are far less intensive than previous methods, allowing for the modeling of octave-spanning combs with hundreds of spectral modes on a consumer grade computer in a matter of seconds. We also show that the results obtained from the proposed model provide significant insights into Kerr combs. In particular, we highlight how localized dissipative structures known as temporal cavity solitons (CSs) [7] are stable stationary solutions of the governing equation, and how specific comb features can be intuitively described in terms of CS propagation. We expect the reported technique to become an invaluable tool for the understanding and tailoring of nonlinear

optical phenomena in microring resonators.

We consider a typical microresonator configuration (Fig. 1): a continuous-wave (cw) driving field E_{in} with power $P_{\text{in}} = |E_{\text{in}}|^2$ is coherently added to the light wave circulating in the resonator through a coupler with power transmission coefficient θ . The remaining port of the coupler is used to extract the output field. Mathematically the intracavity field $E^{(m+1)}(0, \tau)$ at the beginning of the $(m+1)^{\text{th}}$ roundtrip can be related to the field $E^{(m)}(L, \tau)$ at the end of the m^{th} roundtrip as:

$$E^{(m+1)}(0, \tau) = \sqrt{\theta} E_{\text{in}} + \sqrt{1 - \theta} E^{(m)}(L, \tau) e^{i\phi_0}, \quad (1)$$

where τ is the time, L the roundtrip-length of the resonator, and ϕ_0 the linear phase accumulated by the intracavity field with respect to the the pump field over one roundtrip.

Assuming that light propagates in a single spatial mode of the microresonator, the evolution of the field through one roundtrip of the resonator is governed by the well-known (generalized) NLS equation:

$$\frac{\partial E(z, \tau)}{\partial z} = -\frac{\alpha_i}{2} E + i \sum_{k \geq 2} \frac{\beta_k}{k!} \left(i \frac{\partial}{\partial \tau} \right)^k E + i \gamma |E|^2 E. \quad (2)$$

Here α_i is the linear absorption coefficient inside the resonator, $\beta_k = d^k \beta / d\omega^k|_{\omega=\omega_0}$ the dispersion coefficients associated with the Taylor series expansion of the propagation constant $\beta(\omega)$ about the center frequency ω_0 of the driving field, and $\gamma = n_2 \omega_0 / (c A_{\text{eff}})$ the nonlinear coefficient with n_2 the nonlinear refractive index and A_{eff} the effective modal area of the resonator mode.

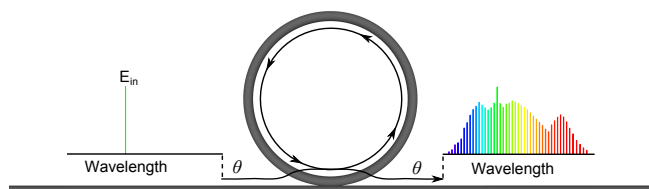


Fig. 1. (Color online) Schematic of the ring configuration.

The boundary conditions Eq. (1) combined with the NLS Eq. (2) form an infinite-dimensional map that describes completely the dynamics of a ring resonator. In low loss structures, the field varies only slightly between consecutive roundtrips, making direct simulations of these equations very slow [3]. In these conditions, however, it is well known that Eqs. (1)–(2) can be averaged into an externally driven NLS equation (see, e.g., [8]),

$$t_R \frac{\partial E(t, \tau)}{\partial t} = \left[-\alpha - i\delta_0 + iL \sum_{k \geq 2} \frac{\beta_k}{k!} \left(i \frac{\partial}{\partial \tau} \right)^k + i\gamma L |E|^2 \right] E + \sqrt{\theta} E_{\text{in}}, \quad (3)$$

where t_R is the roundtrip time, $\alpha = (\alpha_i + \theta)/2$ describes the total cavity losses, and $\delta_0 = 2\pi l - \phi_0$ is the detuning with l the order of the cavity resonance closest to the driving field. The continuous variable t measures the *slow time* of the cavity, and can be linked to the roundtrip index as $E(t = mt_R, \tau) = E^{(m)}(0, \tau)$. Equation (3) (with $\beta_k = 0$ for $k \geq 3$) is formally identical to the mean-field LL model of a diffractive cavity, and coincides with the master equation of [5]. It has also been extensively used for the description of passive cavities constructed of single-mode fibers [6–12]. In particular, spatial pattern formation and the so-called modulation instability (MI) studied in some of these earlier works can be directly connected to frequency comb generation [6, 9, 11]. MI was also shown to occur in the normal GVD regime in presence of cavity boundary conditions [8, 10], which is also directly relevant to combs. We must also note that the expressions of the characteristic bistable response of the LL model as well as that of the intracavity MI gain [8] in fact coincide after normalization with corresponding results obtained from the coupled-mode equations of [4], suggesting an intrinsic link between the two approaches.

The generalized LL Eq. (3) holds in the limit of high finesse cavities $\mathcal{F} \gg 1$. For typical microresonators with Q factors of 10^8 the finesse $\mathcal{F} \sim 10^5$. Also, dispersion must be “weak” over one roundtrip, $\sum_{k \geq 2} \beta_k L \Delta\omega^k / k! \lesssim \pi$, where $\Delta\omega$ is the (angular) spectral width of the generated comb. This condition was found to be satisfied *a posteriori* for all the results discussed below, thereby asserting the validity of Eq. (3) for the description of microresonators. The LL equation has two substantial advantages compared to the infinite dimensional map Eqs. (1)–(2). On the one hand, Eq. (3) can be numerically integrated with the split-step Fourier method using an integration step corresponding to *multiple simultaneous roundtrips*, significantly reducing the computational burden in obtaining steady state solutions. On the other hand, the steady state solutions can be obtained directly by setting $\partial E / \partial t = 0$ and looking for the roots of the right-hand-side of Eq. (3). Although the latter approach does not yield insights into the dynamics of comb formation, it is computationally orders of magnitude more efficient than split-step integration. In what follows we restrict our attention to the stationary solu-

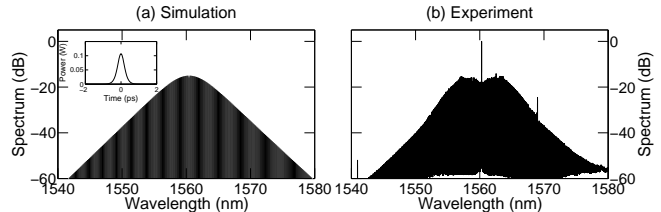


Fig. 2. (a) Steady state solution of Eq. (3) for a critically-coupled, 3.8 mm diameter MgF₂ whispering gallery mode resonator with a 40 μm mode-field diameter and a loaded $Q = 1.95 \cdot 10^9$ as approximated from [13]. FSR = 18.2 GHz; $\gamma = 0.032 \text{ W}^{-1}\text{m}^{-1}$; $\beta_2 = -13 \text{ ps}^2 \text{ km}^{-1}$; $\alpha = \theta = 1.75 \cdot 10^{-5}$; $P_{\text{in}} = 55.6 \text{ mW}$; $L = 11.9 \text{ mm}$; $\delta_0 = 0.0012$. (b) Corresponding experimental spectrum after [13].

tions, and present results obtained by finding the roots of Eq. (3) using a multidimensional Newton-Raphson method. Computation of derivatives is based on Fourier transforms and the span of the temporal window coincides with t_R , meaning the samples of our frequency grid are spaced by the free-spectral range, $\text{FSR} = 1/t_R$.

As a first example, we plot in Fig. 2(a) the spectrum of a stable steady-state solution of Eq. (3) obtained with simulation parameters (see caption) approximating the experimental values of [13]. We note that some of these parameters have large uncertainties but this does not invalidate our conclusions. Figure 2(b) is the corresponding experimental spectrum, and clearly excellent agreement is observed. We also show the temporal profile of the solution as an inset of Fig. 2(a) so as to highlight that the intracavity field corresponds to a ~ 400 fs-duration pulse with a peak power of 100 mW atop a weak cw background. It is well-known that the LL equation possesses such localized-CS solutions repeating at the cavity repetition rate thus forming a frequency comb in the spectral domain [7, 12]. In fact, in solving Eq. (3), we have not found any type of stable steady-state comb solutions not made up of single or multiple CSs. This strongly suggests that frequency combs generated in microcavities generally correspond to regular trains of CSs which is in good accordance with recent autocorrelation measurements and other studies [2, 5].

Our next example (Fig. 3) is an octave-spanning comb for which higher-order dispersion is important. The simulation parameters are approximated from the experiment of [14] and are listed in the caption. Again we observe an excellent agreement between the stable steady-state solution of Eq. (3) plotted in Fig. 3(a) and the experimental measurements (see Fig. 2 in [14]). At this point we must emphasize that, despite the large number of spectral modes, the computation time in obtaining the results shown both in Figs. 2(a) and 3(a) was of the order of seconds on a standard computer. It is precisely this unprecedented speed that is the key advantage of our technique. In fact, to our knowledge, the spectrum shown in Fig. 3(a) constitutes the first Kerr comb simulation result spanning over an optical octave (~ 130 THz), and also contains the largest number of optical modes (~ 600) obtained from a theoretical model.

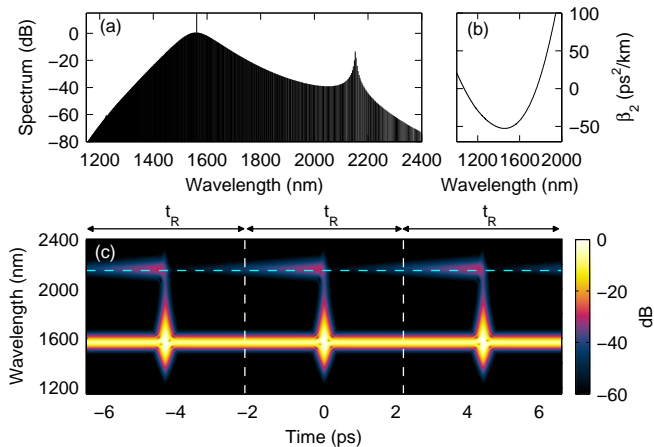


Fig. 3. (Color online) (a) Steady-state solution of Eq. (3) with parameters mimicking a critically-coupled, 200 μm diameter silicon nitride resonator with a loaded $Q = 3 \cdot 10^5$ approximated from [14]. Dispersion as per (b); FSR = 226 GHz; $\gamma = 1 \text{ W}^{-1}\text{m}^{-1}$; $\alpha = \theta = 0.009$; $P_{\text{in}} = 755 \text{ mW}$; $L = 628 \mu\text{m}$; $\delta_0 = 0.0534$. (c) Time-frequency representation of the simulation result calculated using a 100 fs gate function. Subsequent roundtrips are separated by vertical lines whilst the horizontal line indicates the predicted Čerenkov wavelength.

A particular feature seen in Fig. 3(a) is the strong narrowband low-frequency component centered about 2150 nm. A similar feature can be witnessed in the corresponding experimental measurements [14], and also in other previous experiments (see, e.g., Fig. 1 in [15]). We interpret this component as a Čerenkov-like resonant dispersive wave (DW) emitted by the CS circulating in the microresonator [16]. To show this explicitly, we plot in Fig. 3(c) the time-frequency representation of the intracavity electric field. Here we exploit the periodic boundary conditions, and expand the fast temporal axis across three cavity roundtrips. We can clearly see how the intracavity field consists of a train of pulses atop a cw background (i.e., CSs) and we can identify the narrowband 2150 nm component as DWs emitted by individual CSs. This is further highlighted by the dashed horizontal line in Fig. 3(c) which indicates the predicted wavelength λ_{DW} of a Čerenkov-wave. Specifically, neglecting the nonlinear contribution, the pertinent phase-matching condition governing the resonant DW is $\beta(\omega_{\text{DW}}) = \beta(\omega_{\text{CS}}) - \beta_1(\omega_{\text{CS}}) \cdot (\omega_{\text{CS}} - \omega_{\text{DW}})$ [16], where $\omega_{\text{DW}} = 2\pi c/\lambda_{\text{DW}}$ and ω_{CS} are the central (angular) frequencies of the DW and the CS, respectively. With our numerical parameters, this condition yields $\lambda_{\text{DW}} = 2149 \text{ nm}$, in excellent agreement with the observed spectral peak in Fig. 3(a). Because a (cavity) soliton in the anomalous GVD regime can only excite DWs in the normal GVD regime, our observations suggest that the ubiquitous asymmetry of Kerr combs towards the normal GVD regime may in fact be explained by the excitation of resonant DWs by CSs in the anomalous GVD region in a way akin to supercontinuum generation [16]. Finally, we note that DW emission has recently been described in terms of cascaded four-wave mixing, which further highlights its relevance to Kerr combs [17].

In conclusion, we have used a generalized LL equation to model microresonator Kerr frequency combs. It can be solved with a Newton-Raphson solver, providing results in a matter of seconds, much faster than any other technique, even in the case of octave-spanning combs with hundreds of modes. Our results are in good agreement with experiments and indicate that Kerr frequency combs are associated in the temporal domain with CSs [7] and associated DWs. CSs are well known localized dissipative structures which have been studied extensively in the past, in particular in the spatial domain [9, 12], so we anticipate that the LL model will provide both a deeper understanding to Kerr frequency combs and computational efficiency. The Newton method also provides information about dynamical instabilities of Kerr combs through an eigenvalue analysis of the Jacobian of the system, which is obtained at no extra cost. Some of our preliminary results highlight the presence of Hopf bifurcations associated with breathing CSs, i.e., combs with periodically modulated features, which have been reported recently.

We thank Dr I. S. Grudinin for kindly providing experimental data. We also acknowledge support from the Marsden Fund of The Royal Society of New Zealand.

References

1. T. J. Kippenberg, R. Holzwarth, and S. A. Diddams, *Science* **332**, 555 (2011).
2. F. Ferdous, H. Miao, D. E. Leaird, K. Srinivasan, J. Wang, L. Chen, L. T. Varghese, and A. M. Weiner, *Nat. Photon.* **5**, 770 (2011).
3. I. H. Agha, Y. Okawachi, and A. L. Gaeta, *Opt. Express* **17**, 16209 (2009).
4. Y. K. Chembo and N. Yu, *Phys. Rev. A* **82**, 033801 (2010).
5. A. B. Matsko, A. A. Savchenkov, W. Liang, V. S. Ilchenko, D. Seidel, and L. Maleki, *Opt. Lett.* **36**, 2845 (2011).
6. L. A. Lugiato and R. Lefever, *Phys. Rev. Lett.* **58**, 2209 (1987).
7. F. Leo, S. Coen, P. Kockaert, S.-P. Gorza, P. Emplit, and M. Haelterman, *Nat. Photon.* **4**, 471 (2010).
8. M. Haelterman, S. Trillo, and S. Wabnitz, *Opt. Commun.* **91**, 401 (1992).
9. A. J. Scroggie, W. J. Firth, G. S. McDonald, M. Tlidi, R. Lefever, and L. A. Lugiato, *Chaos, Solitons & Fractals* **4**, 1323 (1994).
10. S. Coen and M. Haelterman, *Opt. Lett.* **24**, 80 (1999).
11. S. Coen and M. Haelterman, *Opt. Lett.* **26**, 39 (2001).
12. L. A. Lugiato, *IEEE J. Quantum Elec.* **39**, 193 (2003).
13. I. S. Grudinin, L. Baumgartel, and N. Yu, *Opt. Express* **20**, 6604 (2012).
14. Y. Okawachi, K. Saha, J. S. Levy, Y. H. Wen, M. Lipson, and A. L. Gaeta, *Opt. Lett.* **36**, 3398 (2011).
15. M. A. Foster, J. S. Levy, O. Kuzucu, K. Saha, M. Lipson, and A. L. Gaeta, *Opt. Express* **19**, 14233 (2011).
16. J. M. Dudley, G. Genty, and S. Coen, *Rev. Mod. Phys.* **78**, 1135 (2006).
17. M. Erkintalo, Y. Q. Xu, S. G. Murdoch, J. M. Dudley, and G. Genty, *Phys. Rev. Lett.*, accepted (2012).

References with titles

1. T. J. Kippenberg, R. Holzwarth, and S. A. Diddams, “Microresonator-based optical frequency combs,” *Science* **332**, 555–559 (2011).
2. F. Ferdous, H. Miao, D. E. Leaird, K. Srinivasan, J. Wang, L. Chen, L. T. Varghese, and A. M. Weiner, “Spectral line-by-line pulse shaping of on-chip microresonator frequency combs,” *Nature Photonics* **5**, 770–776 (2011).
3. I. H. Agha, Y. Okawachi, and A. L. Gaeta, “Theoretical and experimental investigation of broadband cascaded four-wave mixing in high-Q microspheres,” *Optics Express* **17**, 16209–16215 (2009).
4. Y. K. Chembo and N. Yu, “Modal expansion approach to optical-frequency-comb generation with monolithic whispering-gallery-mode resonators,” *Physical Review A* **82**, 033801/1–18 (2010).
5. A. B. Matsko, A. A. Savchenkov, W. Liang, V. S. Ilchenko, D. Seidel, and L. Maleki, “Mode-locked Kerr frequency combs,” *Optics Letters* **36**, 2845–2847 (2011).
6. L. A. Lugiato and R. Lefever, “Spatial dissipative structures in passive optical systems,” *Physical Review Letters* **58**, 2209–2211 (1987).
7. F. Leo, S. Coen, P. Kockaert, S.-P. Gorza, P. Emplit, and M. Haelterman, “Temporal cavity solitons in one-dimensional Kerr media as bits in an all-optical buffer,” *Nature Photonics* **4**, 471–476 (2010).
8. M. Haelterman, S. Trillo, and S. Wabnitz, “Dissipative modulation instability in a nonlinear dispersive ring cavity,” *Optics Communications* **91**, 401–407 (1992).
9. A. J. Scroggie, W. J. Firth, G. S. McDonald, M. Tlidi, R. Lefever, and L. A. Lugiato, “Pattern formation in a passive Kerr cavity,” *Chaos, Solitons & Fractals* **4**, 1323–1354 (1994).
10. S. Coen and M. Haelterman, “Competition between modulational instability and switching in optical bistability,” *Optics Letters* **24**, 80–82 (1999).
11. S. Coen and M. Haelterman, “Continuous-wave ultrahigh-repetition-rate pulse-train generation through modulational instability in a passive fiber cavity,” *Optics Letters* **26**, 39–41 (2001).
12. L. A. Lugiato, “Introduction to the feature section on cavity solitons: an overview,” *IEEE Journal of Quantum Electronics* **39**, 193–196 (2003).
13. I. S. Grudinin, L. Baumgartel, and N. Yu, “Frequency comb from a microresonator with engineered spectrum,” *Optics Express* **20**, 6604–6609 (2012).
14. Y. Okawachi, K. Saha, J. S. Levy, Y. H. Wen, M. Lipson, and A. L. Gaeta, “Octave-spanning frequency comb generation in a silicon nitride chip,” *Optics Letters* **36**, 3398–3400 (2011).
15. M. A. Foster, J. S. Levy, O. Kuzucu, K. Saha, M. Lipson, and A. L. Gaeta, “Silicon-based monolithic optical frequency comb source,” *Optics Express* **19**, 14233–14239 (2011).
16. J. M. Dudley, G. Genty, and S. Coen, “Supercontinuum generation in photonic crystal fiber,” *Reviews of Modern Physics* **78**, 1135–1184 (2006).
17. M. Erkintalo, Y. Q. Xu, S. G. Murdoch, J. M. Dudley, and G. Genty, “Cascaded phase-matching and nonlinear symmetry breaking in fiber frequency combs,” *Phys. Rev. Lett.*, accepted (2012).